Site Affinity Effects upon Charge Injection into Siloxane-based Monolayers

4 AUTHORS, INCLUDING:

Olena Zenkina
University of Ontario Institute of Technology
26 PUBLICATIONS   400 CITATIONS

SEE PROFILE

Atindra D Shukla
Dharmsinh Desai University
36 PUBLICATIONS   590 CITATIONS

SEE PROFILE

# Site Affinity Effects upon Charge Injection into Siloxane-based Monolayers

Hagai Cohen,*,† Olena V. Zenkina,‡ Atindra D. Shukla,‡ and Milko E. van der Boom*,‡

Department of Chemical Research Support, and Department of Organic Chemistry,
Weizmann Institute of Science, 76100 Rehovot, Israel

Received: November 20, 2005

Submolecular electrical information is successfully derived by applying element-specific, chemically resolved electrical measurements to a covalently bound stilbazole-based monolayer on a silicon substrate. Pronounced affinity effects are found in the response of adjacent atomic sites to external charge injection, accompanied by intramolecular polarization variations. These noncontact electrical read-out capabilities may provide a first entry toward the realization of organic devices based on submolecular electrical units.

Ratner and Aviram proposed molecular rectifier in 1974 inspired many and has catalyzed an enormous interest in molecular electronics.[1] Much progress has been made on understanding electronic processes such as molecular charge transport in organic thin films.[2−16] Several methods, including shear force-based scanning probe microscopy (SPM),[4] atomic force electrochemical microscopy (AFM-SECM),[11] and cyclic voltammetry using mercury contact electrodes[2,3,6] have been used to study the abovementioned phenomena. Until now, fundamental questions such as the distribution of injected charge within organic thin films are difficult to address. Charging induced line-shifts in X-ray photoelectron spectroscopy (XPS)[17−21] and controlled surface charging (CSC)[22,23] were used to determine positions of different elements, while a recently developed method, chemically resolved electrical measurements (CREM), has been proposed as a direct probe of electrical properties at atomically defined sites with no physical contact between the device setup, power supply, and voltmeter.[10,24] We demonstrate here noncontact, element-specific submolecular CREM, using a stilbazole-based monolayer. Prominent affinity effects and intramolecular polarization variations are observed in adjacent atomic sites upon charge injection.

A fundamental understanding of thin films and controlling thin film electronic properties are crucial for interface design and the formation of organic-based devices. Monolayer design, intermolecular interactions, substrate effects and electrode contacts have a significant influence on structure−function relationships. CREM application to submolecular studies of monolayers, offers ample possibilities for molecular electronics, including element specific $I-V$ measurements. The chemical resolution can be exploited in monolayers of compound **1** using the line-shifts of the various elements that occur under varying the electrical conditions as submolecular markers. Stilbazole-based multilayers have been integrated into prototype electrooptic modulators and organic field effect transistors.[25,26] The trimethoxysilane moiety of **1** provides strong, covalent binding

to hydrophilic substrate surfaces, whereas the pyridinium and CF_3 units are introduced as spectroscopic probes.
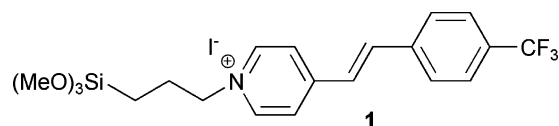
Reaction of 4-[2-(4-trifluoromethyl-phenyl)-vinyl]-pyridine with an 4-fold excess of 3-iodo-*n*-propyl-1-trimethoxysilane in dry THF under N_2 at 85 °C in a glass pressure vessel resulted in the quantitative formation of the corresponding pyridinium salt **1**. The new compound **1** has been isolated and fully characterized by a combination of ^1H, $^{13}C\{^1H\}$, and $^{19}F\{^1H\}$ NMR spectroscopy, mass spectrometry, UV−vis measurements, and elemental analysis. Freshly cleaned silicon substrates were treated with a dry THF solution of **1** (1 mM) at 85 °C for 24 h in a sealed glass pressure vessel under N_2 with exclusion of light. The colored substrates were rinsed repeatedly with dry THF and acetone with sonication for 5 min, then dried under a stream of N_2. Subsequently, the films were cleaned with a CO_2 snowjet.[27] The new covalent assembled monolayers adhere strongly to the hydrophilic substrates, as demonstrated by insolubility in common organic solvents and inability to be removed from the substrates by Scotch tape. The functionalized substrates were stored under N_2 with exclusion of light at room temperature. The monolayers were characterized by a series of physicochemical techniques, including transmission optical (UV−vis) spectroscopy, aqueous contact angle (CA) measurements, atomic force microscopy (AFM), and XPS. Transmission UV−vis spectroscopy of monolayer **1** showed a maximum absorption band at 335 nm, which is nearly identical to **1** in solution. The advancing aqueous CA value, $\theta_a \approx 73°$, is in range with CA values observed for structurally related stilbazole-based monolayers.[28] AFM measurements show a uniform surface without grains or pinholes, and a root-mean-square (rms) surface roughness of ∼0.2 nm for 0.5 μm × 0.5 μm scan areas (see Supporting Information for details).

XPS measurements on monolayers grown on highly doped p-Si substrates reveal the expected elemental composition,

* Corresponding authors. E-mail: hagai.cohen@weizmann.ac.il, milko.vanderboom@weizmann.ac.il.
† Department of Chemical Research Support.
‡ Department of Organic Chemistry.

Letters

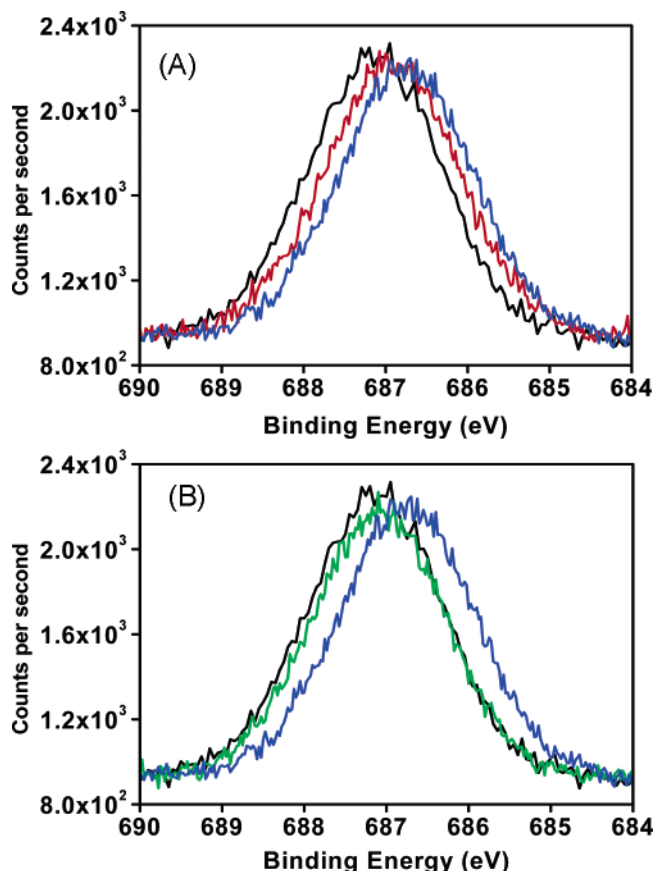*J. Phys. Chem. B, Vol. 110, No. 4, 2006* **1507**

Figure 1. Spectral line shifts of the F(1s) signals under varying incoming electron flux. (A) Stepwise increase of the negative current. The black, red, and blue spectra are recorded at +0.27 nA (eFG off), −7.7 nA, and at −14.0 nA, respectively. (B) Reversibility check. The black and green spectra represent the starting and end points (eFG off). The blue trace presents the spectrum under a negative current of −14.0 nA.

Figure 2. Representative chemically resolved $I-V$ measurements on monolayer **1**. Each measurement consists of five operating stages at the eFG: (1) off, +0.24 nA, (2) −7.7 nA, (3) −14 nA, (4) −5.8 nA, and (5) off, +0.28 nA. Note that (1) and (5) consist of positive charging due to the outgoing flux of X-ray ejected photoelectrons. The colored dotted lines are drawn as guides for the eye. (●) C^F, carbon atom of CF_3 unit (*) N, nitrogen atom of the pyridinium unit, (▲) C, aromatic and aliphatic carbon atoms, (■) F, fluorine atoms of the CF_3 unit.
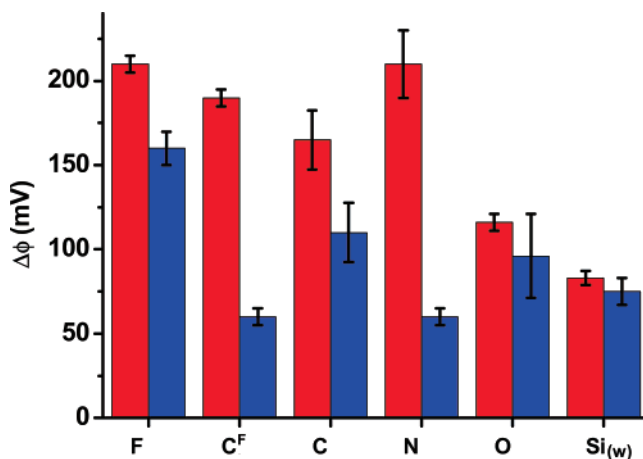
Figure 3. Chemically resolved potential changes, $\Delta\phi$: $Si_{(w)}$ and O represent the substrate wafer and the oxide layer, while the other elements probe specific molecular sites. The red columns present the average $\Delta\phi$ of the first and last steps in the electrical scan (between eFG off and −7.7 nA, and between −5.8 nA and eFG off, see Figure 2); The blue columns present average $\Delta\phi$ values for the second and third steps of the $I-V$ measurement (with eFG currents of −7.7 nA and −14 nA, and back to −5.8 nA). Error bars correspond to the experimental irreversible spectral drifts.

corrected for electron attenuation. The I(3d) signal is very weak or absent and excess of some carbon and oxygen is frequently observed. The characteristic pyridinium N(1s) signal appears at 401.8 eV. The N/F concentration ratio, ∼1:3, is as expected. Angle resolved XPS (ARXPS) derived monolayer thickness is ∼8.7 Å. This value is similar to reported thicknesses for structurally related monolayers.[28] The ARXPS data further point at a uniform film thickness, namely a low concentration of holes or disorder in the molecular alignment.

The electrical setup consists of a back contact to a Keithley 587 picoampermeter and two noncontact components: a Kratos AXIS−HS spectrometer with monochromatized Al(kα) radiation, acting as a multichannel voltmeter, and an electron flood gun (eFG) serving as the power supply (= electron source). An improved accuracy in line shifts evaluation can be achieved (±10 mV, depending on noise level and spectra stability) by correlating the full line shape (100−200 data points) other than its peak position.[10] Repetitive scans on fixed spots showed a slow decrease of the fluorine signal and an even slower reduction of the quarternized nitrogen on a time scale of several hours.[29] Sample cooling to about −50 °C effectively slowed these processes. The here-presented low temperature CREM data correspond to relatively quick scans (5−20 min), performed on fresh spots with applying reversibility checks.

Representative spectra of F(1s) under varying the eFG current are shown in Figures 1a,b. The line shifts directly reflect changes in the electrostatic potential at corresponding atomic sites while reversibility is maintained.
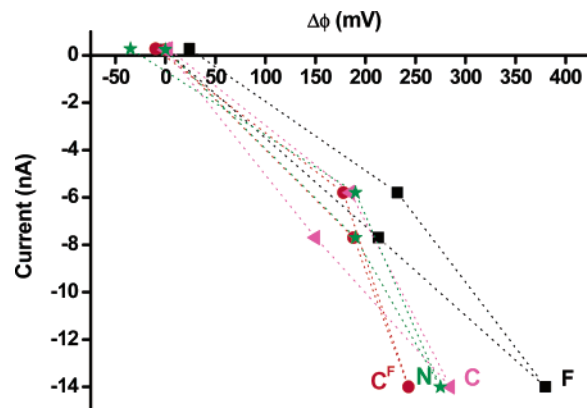
$I-V$ measurements based on the XPS line shifts of the monolayer elements are presented in Figure 2. The zero of the potential scale refers to the initial conditions (eFG off). The electrical steps, as determined by the input current, are roughly equal, but those associated with "switching on/off" of the eFG involve finite positive charging as well. The monolayer stability restricts the number of data points that can be collected during each $I-V$ measurement. Nevertheless, the different responses of the various submolecular sites under identical charging conditions are apparent.

A more convenient comparison of the electrical data for the various elements is depicted in Figure 3, separating the two qualitatively different charging steps shown in Figure 2.

The ability to directly measure potential changes at the submolecular level is an important feature of CREM. For instance, a comparison of the F vs C^F line-shift reveals significant differences in local potential changes at specific adjacent sites. The $\Delta\phi$ of the C^F atom is smaller by a factor

>2.5 from that of its neighboring F atoms under negative charging conditions (the blue columns). This difference across a 1.4 Å distance correlates with the larger electron affinity of fluorine, demonstrating the presence of strong polarization effects within the CF_3 moiety. The CREM-enhanced polarization effect is the molecular phenomenon that gives rise to the observed potential change. Obviously, injecting extra negative charge into the fluorine atoms should induce repulsion of electron density away from the adjacent carbon atom. This would locally reduce the electrical potential, as indeed probed via the C^F signal. Note that the blue C^F column is even smaller than the ones of the substrate signals ($Si_{(w)}$, O), pointing at the evolution of positive space charge around the C^F site under injection of negative external charges. This provides additional support for the pronounced polarization of the CF_3 group. Enhanced polarization effects around the quarternized nitrogen might be attributed to neighboring counterions and the charge delocalization within the pyridine moiety. Complementary CREM experiments on various systems,[10,24] have not shown any indication for shifts that are core-level dependent, suggesting that the electrically induced line shifts can indeed be used as a reliable probe of local electrical potentials.

In conclusion, direct detection of electrical properties at submolecular sites within siloxane-based monolayers has been demonstrated. The site specific potential variations reveal fine details in the molecular response to external charge injection, proposing a unique means for exploring organic systems. Site affinity effects and redistribution of space charges across CF_3 groups were identified. CREM application to other organic films (e.g., porphyrin[30] or ferrocene systems) and further refinement of the experimental conditions[10] may provide a novel route toward the realization of devices based on submolecular electrical units.

Supporting Information Available: Formation and characterization data of compound **1** and monolayer **1**. AFM image of monolayer **1** on silicon (Figure S1) and UV/vis spectra of compound **1** in solution and monolayer **1** (Figure S2). This material is available free of charge via the Internet at http://pubs.acs.org.

References and Notes

(1) Aviram, A.; Ratner, M. A. *Chem. Phys. Lett.* **1974**, *29*, 277.

(2) Salomon, A.; Cahen, D.; Lindsay, S.; Tomfohr, J.; Engelkes, V. B.; Frisbie, C. D. *Adv. Mater.* **2003**, *15*, 1881.

(3) Cahen, D.; Hodes, G. *Adv. Mater.* **2002**, *14*, 789.

(4) Fan, F.-R. F.; Yao, Y.; Cai, L.; Cheng, L.; Tour, J. M.; Bard, A. J. *J. Am. Chem. Soc.* **2004**, *126*, 4035.

(5) Metzger, R. M. *Chem. Rev.* **2003**, *103*, 3803.

(6) Tran, E.; Rampi, M. A.; Whitesides, G. M. *Angew. Chem., Int. Ed.* **2004**, *43*, 3835.

(7) Zaslavsky, D.; Pakoulev, A.; Burtman, V. *J. Phys. Chem. B* **2004**, *108*, 15815.

(8) Zangmeister, C. D.; Robey, S. W.; van Zee, R. D.; Yao, Y.; Tour, J. M. *J. Phys. Chem. B* **2004**, *108*, 16187.

(9) Gershewitz, O.; Grinstein, M.; Sukenik, C. N.; Regev, K.; Ghabboun, J.; Cahen, D. *J. Phys. Chem. B* **2004**, *108*, 664.

(10) Cohen, H. *Appl. Phys. Lett.* **2004**, *85*, 1271.

(11) Abbou, J.; Anne, A.; Demaille, C. *J. Am. Chem. Soc.* **2004**, *126*, 10095.

(12) Schreiber, F. *J. Phys.: Condens. Matter* **2004**, *16*, R881.

(13) Holmlin, R. E.; Ismagilov, R. F.; Haag, R.; Mujica, V.; Ratner, M. A.; Rampi, M. A.; Whitesides, G. M. *Angew. Chem., Int. Ed.* **2001**, *40*, 2316.

(14) Onipko, A. I.; Berggren, K.-F.; Klymenko, Y. O.; Malysheva, L. I.; Rosink, J. J. W. M.; Geerlings, L. J.; van der Drift, E.; Radelaar, S. *Phys. Rev. B* **2000**, *61*, 11118.

(15) Seminario, J. M.; Zacarias, A. G.; Tour, J. M. *J. Am. Chem. Soc.* **1998**, *120*, 3970.

(16) Ghosh, A. W.; Damle, P. S.; Datta, S.; Nitzan, A. *MRS Bull.* **2004**, *29*, 391.

(17) Lau, W. M. *Appl. Phys. Lett.* **1989**, *54*, 338.

(18) Miller, J. D.; Harris, W. C.; Zajac, G. W. *Surf. Interface Anal.* **1993**, *20*, 977.

(19) Barr, T. L. *J. Vac. Sci. Technol.* **1989**, *A 7*, 1677.

(20) Cazaux, J. *J. Electron Spectrosc. Relat. Phenom.* **1999**, *105*, 155.

(21) Hofmann, S. *Practical Surface Analysis*, 2 ed.; Briggs, D., Seah, M. P., Eds.; Wiley: New York, 1990; Vol. 1, p 143.

(22) Shabtai, K.; Rubinstein, I.; Cohen, S. R.; Cohen, H. *J. Am. Chem. Soc.* **2000**, *122*, 4959.

(23) Doron-Mor, I.; Hatzor, A.; Vaskevich, A.; van der Boom-Moav, T.; Shanzer, A.; Rubinstein, I.; Cohen, H. *Nature* **2000**, *406*, 382.

(24) Cohen, H.; Nogues, C.; Zon, I.; Lubomirsky, I. *J. Appl. Phys.* **2005**, *97*, 113701.

(25) Yoon, M.-H.; Facchetti, A.; Marks, T. J. *Proc. Natl. Acad. Sci. U.S.A.* **2005**, *102*, 4678.

(26) Zhao, Y.-G.; Wu, A.; Lu, H.-L.; Chang, S.; Lu, W.-K.; Ho, S. T.; van der Boom, M. E.; Marks, T. J. *Appl. Phys. Lett.* **2001**, *79*, 587.

(27) Chow, B. Y.; Mosley, D. W.; Jacobson, J. M. *Langmuir* **2005**, *21*, 4782.

(28) Shukla, A. D.; Strawser, D.; Lucassen, A. C. B.; Freeman, D.; Cohen, H.; Jose, A. D.; Das, A.; Evmenenko, G.; Dutta, P.; van der Boom, M. E. *J. Phys. Chem. B* **2004**, *108*, 17505.

(29) Frydman, E.; Cohen, H.; Maoz, R.; Sagiv, J. *Langmuir* **1997**, *13*, 5089.

(30) Yerushalmi, R.; Scherz, A.; van der Boom, M. E. *J. Am. Chem. Soc.* **2004**, *126*, 2700.